Heat and Smoke Emission from Tests on the SAFFIRE IV-VI Experiments

David L. Urban[1], Gary A. Ruff[2], Paul Ferkul[3], John Easton[4], Jay Owens[5], Sandra Olson[6], Claire Fortenberry[7]
NASA Glenn Research Center, Cleveland, OH, USA

John Graf[8], Oageng George [9]
NASA Johnson Space Center, Houston, TX, USA

Balazs Toth[10]
ESTEC, Noordwijk, Netherlands

Florian Meyer[11], Christian Eigenbrod[12]
University of Bremen (ZARM), Bremen, Germany

James S. T'ien[13], Ya-Ting T. Liao[14]
Case Western Reserve University, Cleveland, OH, USA

A. Carlos Fernandez-Pello[15]
UC Berkeley, Berkeley, CA, USA

Guillaume Legros[16]
Sorbonne Université & CNES, Paris F-75005, France

Augustin Guibaud[17]
NYU, New York City, NY, USA

Nickolay Smirnov[18]
Moscow State University, Russian Federation

Osamu Fujita[19] and
Hokkaido University, Sapporo, Japan

Ulises Rojas Alva[20], Grunde Jomaas[21]
FRISSBE, ZAG, Ljubljana, Slovenia

The hazardous product release results from seven long-duration low-gravity fire tests are presented. These tests were conducted in low-earth orbit aboard a Cygnus spacecraft where the atmosphere pressure and oxygen concentration were varied to examine the effect of exploration atmosphere conditions. All of the samples were 40 cm wide. Four samples were PMMA and were 18 cm long. Two of these samples burned on both sides and the other two sample were attached to a plate that prevented fire on one side. The other three samples were cotton or a composite cotton/fiberglass blend that were 50 cm long. The cabin concentration of CO and CO_2 were measured continuously in addition to the aerosol concentration. The aerosol concentration was determined using a light scattering device. The heat release from some of the tests was estimated using oxygen consumption calorimetry by measuring the

[1] Branch Chief, Low gravity Exploration Technology (LTX), MS 77-5, 21000 Brookpark Rd, Cleveland, OH, USA.
[2] Saffire Project Manager, Exploration Systems Office,21000 Brookpark Road, Cleveland, OH, USA.
[3] Staff Scientist, Universities Space Research Assoc. (USRA), 21000 Brookpark Road, Cleveland, OH, USA.
[4] Staff Scientist, Case Western Reserve University (CWRU) MS 110-3, 21000 Brookpark Road, Cleveland, OH, USA.
[5] Engineer, USRA, MS 77-5, 21000 Brookpark Road, Cleveland, OH, USA.
[6] Aerospace Engineer, LTX, MS 77-5, 21000 Brookpark Road, Cleveland, OH, USA.
[7] Aerospace Engineer, LTX, MS 77-5, 21000 Brookpark Road, Cleveland, OH, USA.
[8] Aerospace Engineer, Life Support Systems Branch, MS-EC3, 2101 E NASA Pkwy, Houston, TX, USA.
[9] Jacobs Engineering, Project Engineer, ECLSS, JE4EA, 2224 Bay Area Boulevard, Houston, TX 77058.
[10] Payload System Engineer, ESA/ESTEC, Keplerlaan, 2201 Noordwijk, The Netherlands.
[11] Senior Researcher, ZARM, University of Bremen, Am Fallturm 2, 28359 Bremen, Germany.
[12] Researcher, ZARM Univ. of Bremen, Am Fallturm, 28359 Bremen, Germany.
[13] Professor Emeritus, Dept. Mech. and Aero. Engineering, CWRU, Cleveland, OH, USA.
[14] Associate Professor, Dept. Mech. and Aero. Engineering, CWRU, Cleveland, OH, USA.
[15] Professor, Dept. Mech. Engineering, Univ. of California at Berkeley, Berkeley, CA, USA.
[16] Professor, Sorbonne Université & CNES, Paris F-75005, France.
[17] Assistant Professor, Department of MAE, NYU Tandon School of Engineering, NYC, NY, USA
[18] Professor, Mechanics and Mathematics, Moscow M.V. Lomonosov State University, Moscow 119899, Russia
[19] Professor, Hokkaido University, Sapporo, Japan
[20] Senior Researcher, FRISSBE, ZAG, Ljubljana, Slovenia
[21] FRISSBE ERA Chair holder, FRISSBE, ZAG, Ljubljana, Slovenia

oxygen consumption and the production of CO and CO_2. These data were correlated with distributed temperature measurements in the spacecraft and the pressure rise. Overall, the pressure rise and temperature change were small but the smoke particulate rose to substantial levels and the gaseous products also achieved hazardous levels.

Acronyms and Nomenclature

FFD = Far Field Diagnostics
HRR = Heat Release Rate
PMMA = polymethyl methacrylate
SAFFIRE = Spacecraft Fire Safety Demonstration Project
SFU = SAFFIRE Flow Unit
SIBAL = Solid Inflammation Boundary at Low Speed
SMAC = Spacecraft Maximum Allowed Concentration

I. Introduction

DEVELOPMENT of systems and processes to ensure spacecraft fire safety requires an understanding of the behavior of fires in low-gravity and their impact on the habitability of the spacecraft. Prior to the SAFFIRE (Spacecraft Fire Safety Demonstration Project) experiment series, no tests of practical scale fires had been conducted in low gravity. The SAFFIRE series began in 2017 with SAFFIRE I through III occurring between 2017 and 2019 [1] [2]. This series focused primarily on observation of flame spread and growth for large samples of thin materials in flights I and III and a series of smaller samples for flight II [3]. The impact on the spacecraft was deliberately minimized. Subsequently, flights IV-VI studied large, thick, samples that were allowed to burn for longer durations, releasing heat and smoke into the spacecraft cabin. To evaluate the impact of the smoke and heat, a remote diagnostics and filtration system, referred to as the Far Field Diagnostics (FFD) was positioned at the other end of the spacecraft and 6 sensors were distributed across the open volume. Through these tests, it was possible to observe the growth rate of fires on large thick samples and to assess the impact of these fires on the spacecraft. The tests revealed important features of flame spread and growth on both thick [4] [5] and thin [6] materials. These results included delayed extinguishment and reignition of both thick and thin materials [6]; further evidence of the effect of the duct size on spread rate of thin materials; [6] the strong effect of surface structures (ribs) when aligned with the flow direction; [4] and concurrent flame spread on thick materials is suppressed at low flow rates due to the "oxygen shadow." [6]

Understanding the impact of the fire on the spacecraft habitability was a major objective of SAFFIRE IV-VI. The aerosol and gaseous species levels were measured for SAFFIRE IV-V [7] and their transport in the spacecraft was effectively modeled [8]. However, the fire heat release rate (HRR) was not successfully determined for SAFFIRE IV and V, so it was difficult to correlate the products with the fire size. For SAFFIRE VI, the HRR was successfully measured and preliminary analysis showed that, like terrestrial fires, the smoke products can be more hazardous than the heat produced by the fire [9]. This paper extends earlier analysis by considering the time to alarm for a smoke detector and the state of the spacecraft habitability when the alarm is triggered. The primary hazardous products from fires are heat, smoke, HCN, CO and CO_2. NASA requirements limit CO exposure in the Spacecraft Maximum Allowable Concentrations (SMAC) document [10]. For CO the 1-hour SMAC is 425 ppm, and the 24-hour SMAC is 100 ppm. For CO_2, which is a metabolic product that is prevalent in crewed spacecraft, NASA-STD-3001 [11] establishes the limit based on the partial pressure to no more than 3 mm Hg for a 1-hour average. Planning fire response depends on understanding which are the most important hazards. This paper seeks to address that question by examining the CO and CO_2 concentration changes caused by the fire events compared to NASA exposure standards at the time of alarm. These results demonstrate the importance of the hazard from fire smoke projects compared to the heat and pressure rise.

II. Experimental Hardware and Operations

The SAFFIRE flight hardware was installed in the Cygnus spacecraft before launch but was not supplied power until after the Cygnus had departed the International Space Station (ISS). As shown in Figure 1, the SAFFIRE Flow Unit (SFU) was located at the end cone (nadir). The FFD was installed at a middeck locker accommodation area near the hatch(zenith). The 6 remote sensors which measured CO_2 and temperature were located with one in each standoff and one in the end cone (nadir) and one by the hatch (zenith).The vehicle was launched full of cargo which was removed by the ISS crew and replaced with material for disposal. Since the free volume in this configuration was

unknown, the first test sequence on each flight involved the release of a known quantity of CO_2. By measuring the pressure change and tracking the concentration on the remote sensors, the free volume of the spacecraft could be determined. A schematic of the SFU is presented in Figure 2. The flow was driven by a fan at the inlet controlled by the output of a rotary anemometer. In this manner the flow velocity at the entrance of the duct was held constant throughout the test. The CO_2, CO, and O_2 concentrations were measured in the inlet and outlet ducts. Flow straighteners at each end of the 30 cm high, 45 cm wide and 109 cm long duct assured flat, straight, flow profiles. The flow uniformity was verified by smoke traces produced by rosin beads on a heated wire at the beginning and the end of the test sequence.

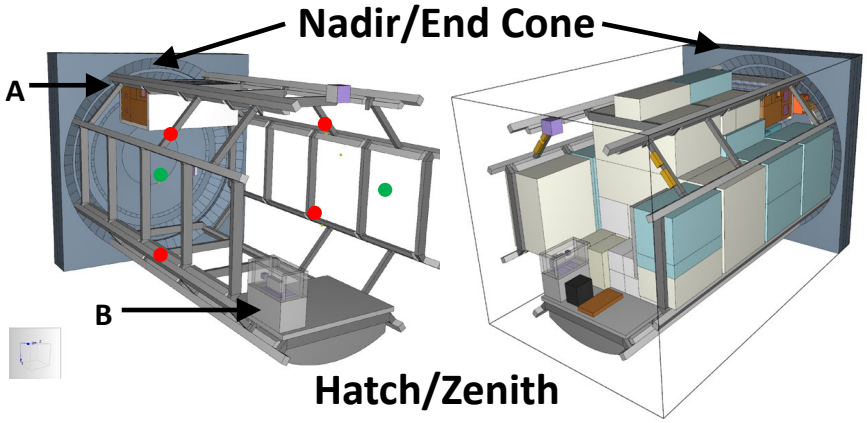


Figure 1. Depiction of the Cygnus spacecraft with SAFFIRE installed. The SAFFIRE Flow Unit (A) and the Far Field Diagnostics (B) are depicted in the vehicle. On the left, there is no cargo installed, and the right has a representation of the descent configuration with the spacecraft loaded with trash. The green dots on the left are the zenith and nadir remote sensors, and the red dots are the remote sensors in the standoffs (the triangular spaces running the length of the spacecraft at the ends of each row of cargo bags).

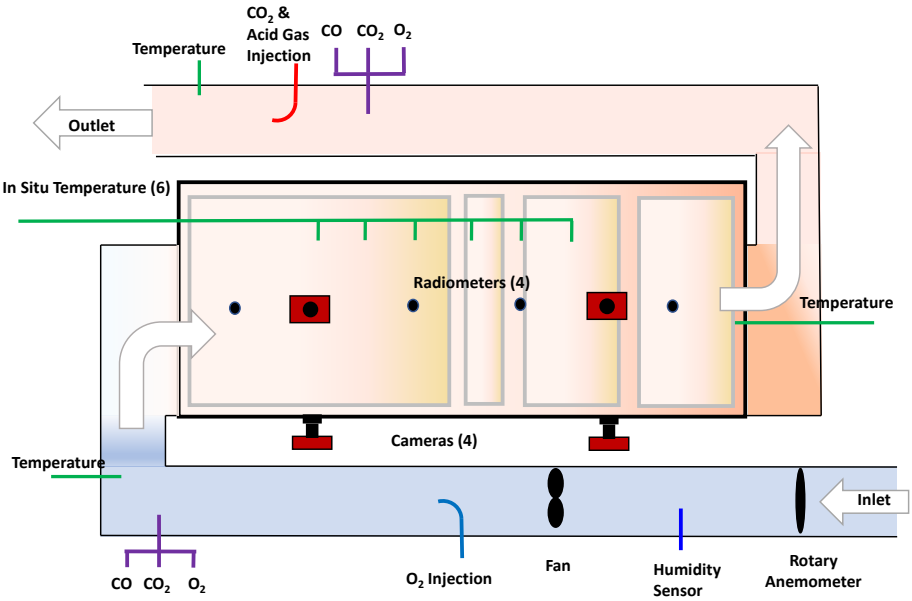


Figure 2. Schematic of SAFFIRE Flow Unit (SFU). Flow enters at the bottom right and is distributed by a plenum on the left before it enters the test section. At the outlet of the test section, (on the right) it enters the outlet duct where gas species measurements are taken that are compared to the inlet.

On each flight, the samples were installed on a single flat frame (Fig. 3) and were ignited individually in separate tests. The flames were imaged by 4 video cameras position to observe the top and edge of the samples. The back side was not imaged. During the burn sequence, the sample surface was briefly illuminated every 2 seconds for approximately 0.1 s by green LEDs. This enabled determination of the length of the pyrolysis zone. The parameters for each test were preprogramed but each test was triggered by ground command to assure continuous telemetry and free drift (not thruster firings) of the spacecraft. Once all of the tests were completed, the data download process began. Due to bandwidth limitations, the video data was compressed and only a reduced number of uncompressed images were downlinked. The spacecraft was initially at the pressure and oxygen concentration of the ISS but on each flight the Cygnus controllers vented the spacecraft to a predetermined pressure and the SFU released oxygen to bring the spacecraft to a targeted level.

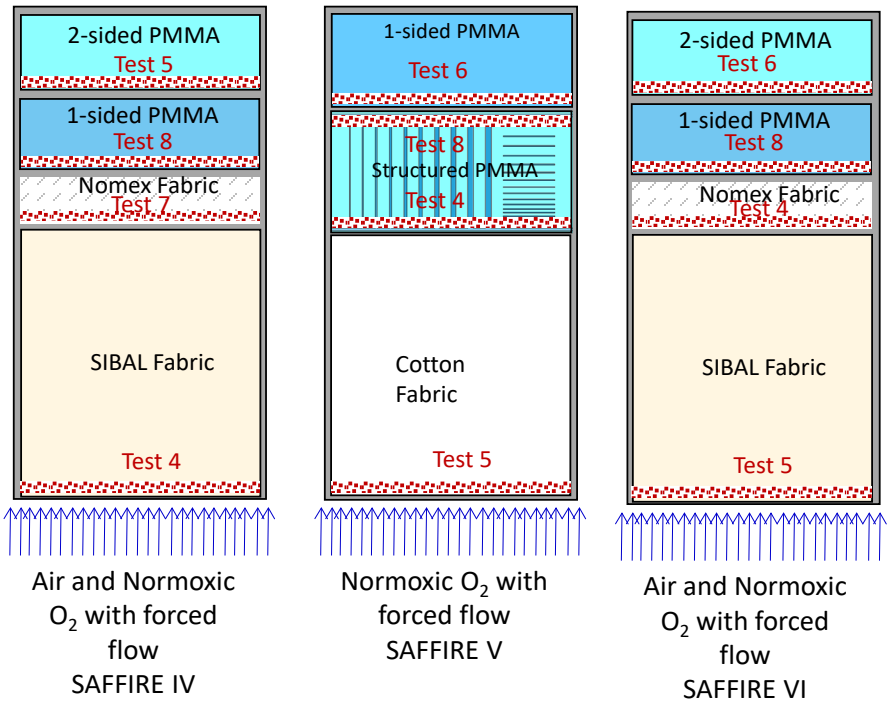


Figure 3: Sample Layouts for SAFFIRE IV-VI. Front view of the sample cards for each flight. The 1-sided PMMA samples were 0.5 cm thick, and the 2-sided samples were 1.0 cm thick. All samples were 40 cm wide. Test numbers account for other test sequences that did not include sample burning.

The FFD (Fig. 4) contained a series of gas sensors as described in more detail by Fortenberry et al. [7]. These included gas sensors to measure CO, CO_2, and O_2; an ionization sensor from a commercial smoke detector; and a TSI DustTrak DRX 8533 which uses light scattering to measure aerosol mass concentration. The location of the FFD was near the inlet of the Cygnus air circulation system so the FFD provided a good assessment of the habitability of the spacecraft, and it could be used to assess when a smoke detector would trigger as the air circulation system sweeps the air toward the intake. This is similar to the ISS where the smoke detectors are in front of air intakes [12].

The flames were tracked from the camera images using a thresholding analysis and using the average flame position over the central third of the flame (neglecting the edge effects). The images were adjusted for the automatic gain of the camera and averaged over 2 second intervals to reduce noise. In general, the trailing edge was very bright (soot) while the leading edge could be dim blue. The flame length was the difference between the average positions of the leading and trailing edges.

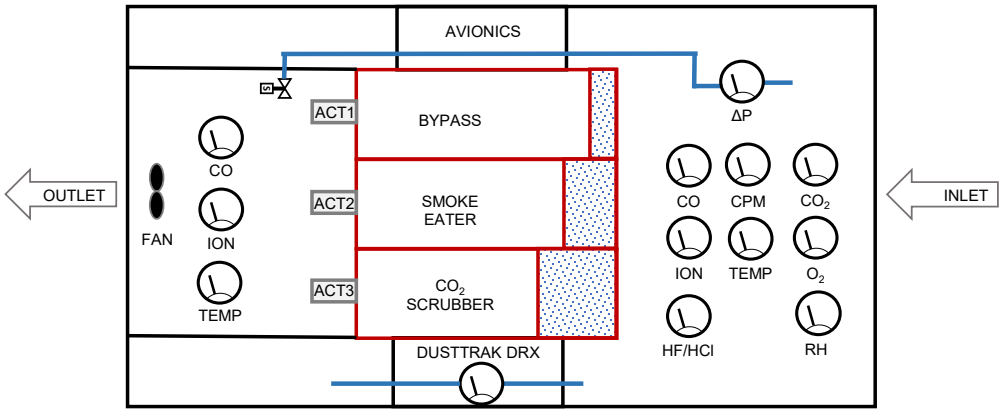


Figure 4. Schematic of the Far Field Diagnostics(FFD). Cabin air enters from the right, and the concentration of gaseous species and smoke aerosol are measured by multiple sensors. The air is directed toward the outlet by one of 3 paths: direct bypass, through a smoke eater or through a CO_2 scrubber. While the sample was burning, the air followed the bypass route. After the sample was extinguished, the smoke eater ran after all tests while the CO_2 scrubber was only operated before SAFFIRE operations and after one test due to its limited capacity.

III. Results and Fire Impact on Habitability

During SAFFIRE IV-VI, there were 4 flat PMMA samples successfully burned and three thin cotton-based samples (cotton t-shirt material and SIBAL fabric) [2]. The structured PMMA tests on SAFFIRE V are discussed in detail by Eigenbrod et al. [4]. The 1-sided PMMA sample for SAFFIRE IV shown in Figure 3 was not ignited due to excessive burning of the 2-sided sample [6]. The operational conditions for these tests along with summary results are presented in Table 1. The flame length of the PMMA samples versus time are shown in Figure 5. Since the ignition time for the one-sided samples was 120 seconds (twice the 2-sided samples) the time axis is referenced to when the ignitor was turned off. This adjustment was only done for this figure. The other figures reference to the experiment's timeline start which is approximately 10 minutes before ignition.

Unlike 1-g upward burning of thick materials such as PMMA, the flames did not spread but remained anchored at the leading edge and only spread as the material regressed. The PMMA samples all showed intervals of very linear flame growth for periods of several minutes. The slopes were generally similar ranging from 0.22 to 0.38 mm/s. This is significantly faster than the observations of the SAFFIRE II, 5 cm wide sample, [5] where the flame grew at less than 0.1 mm/s in air. The 2-sided samples are still growing at the end of the test (around 500 seconds) while the 1-sided samples begin to plateau around 380 s for SAFFIRE V and 420 s for SAFFIRE VI. It is unknown if the 2-sided samples would eventually plateau, longer experiments would be helpful. A plausible explanation for the earlier plateau for the 1-sided samples is the enhanced heat loss through the back side versus the zero-heat loss for the 2-sided samples. In the case of the SAFFIRE II samples, it is likely that heat losses at the edges of the much smaller samples led to the growth limitation. The SAFFIRE thin samples all showed linear flame spread [6]. In comparison, acceleratory flame growth is often seen in normal gravity for upward flame spread on thick fuels. [13] These results suggest that low-gravity flame spread, and growth can be expected to be linear or less and may reach a limiting size.

Heat loss through the back side of a material is relevant in spacecraft applications, where isolated plates burning on both sides are uncommon. The 1-sided configuration simulates a panel or box cover with limited mass behind it. In the test configuration, the back side consisted of a 0.1 mm thick mica sheet (thermal diffusivity ~0.6 mm²/s) followed by a 0.8 mm thick aluminum card (thermal diffusivity ~97 mm²/s). Despite the large difference in diffusivity, the thinness of the mica layer and the high thermal conductivity of the aluminum mean that these back-side materials add less than 1% to the total thermal resistance of the assembly. However, the high diffusivity of aluminum will distribute heat laterally across the back side once the thermal wave has penetrated through the material.

The characteristic thermal penetration time for each layer can be estimated as $\tau = L^2/\alpha$, where L is the thickness and α is the thermal diffusivity. This gives approximately 220 s for the 5 mm PMMA plate (α = 0.11 mm²/s), ~0.017 s for the 0.1 mm mica sheet, and ~0.007 s for the 0.8 mm aluminum card. The combined characteristic time for the full assembly is therefore dominated by the PMMA layer at approximately 220 s, meaning the back-side materials do not meaningfully alter the thermal penetration timescale. For times greater than ~200 s, the thermal wave can be expected to have penetrated the full assembly thickness. The SAFFIRE VI flame growth rate results in Table 1 confirm that back-side heat loss had a significant effect on the growth rate. Since testing all possible configurations is

impractical, 2-sided burn results can be used as a conservative upper-bound estimate of the growth rate for 1-sided applications.

Table 1: Sample materials and test data.
All samples were 40 cm wide in 20 cm/s opposed flow. All PMMA samples were 18 cm long. 1-sided samples were 5 mm thick and 2- sided samples were 10 mm thick. All PMMA samples were preheated for 10 minutes at low ignitor power. SIBAL and Cotton samples were 50 cm long. The Heat Release Rate (HRR) was not successfully measured for flights IV and V. Reported gas concentrations and temperatures were at the FFD. Items in red exceed allowed concentrations.

Flight/Sample	IV-2	V-3	VI-3	VI-4	IV-1	V-2	VI-2
Material	PMMA	PMMA	PMMA	PMMA	SIBAL	Cotton	SIBAL
# of sides burning	2	1	2	1	2	2	2
Pressure (mbar)	1000	745	544	550	980	741	541
Oxygen mol fraction	0.22	0.26	0.30	0.29	0.23	0.28	0.31
Free volume (m^3)	17.9	19	16.7	16.7	17.9	19	16.7
Ignition duration (s)	60	120	60	120	8	8	8
Duration of initial flow (s)	535	480	480	900	200	200	300
Flame length growth rate (mm/s)	0.22	0.26	0.38	0.27	NA	NA	NA
Flame spread rate (mm/s)	NA	NA	NA	NA	3.6	3.4	4.05
Max flame length (mm)	90.8	118	89.9	93.3	NA	NA	NA
Peak HRR (W)	NA	NA	3240	1487	NA	NA	3376
Max CO_2 increase (mm Hg)	1.78	0.78	3.66	3.39	0.97	0.81	1.46
Max CO increase (ppm)	110	55.5	338	309	77.4	74.3	122
Pressure increase (mbar)	1.31	0.25	0.34	0.25	0.33	0.30	0.31
Max temperature increase (°C)	0.23	0.04	0.50	0.25	0.25	0.25	0.29
Time to alarm (s) [aerosol = 2 mg/m^3]	1083	1117	1037	1603	92	146	201
Flame length at alarm (mm)	74	114	73.95	66.9	NA	NA	NA
HRR at alarm (W)	NA	NA	2500	623	NA	NA	3180
CO_2 increase (mm Hg) at alarm	1.28	0.49	1.43	3.09	0.00	0.00	0.04
CO increase (ppm) at alarm	63.2	28.1	105	283	7.9	11.9	57.1

This linear growth rate is an important finding as it suggests that even in high oxygen conditions, low-gravity flame spread and growth will not be acceleratory. Figure 6 shows very close agreement, in the later portion of the test, between the flame length and the radiometer signal for the 2-sided PMMA sample in SAFFIRE VI-3. Flame tracking was halted when the flow was reduced to 5 cm/s at 480 s, as the flame had weakened dramatically. The primary purpose of this low-flow interval was to cool the sample material and ensure extinguishment upon flow termination, thereby avoiding the issues seen in SAFFIRE IV-2 [6]. Rather than dropping immediately, the radiometer measurements continued to rise steadily for an additional 50s. This behavior can be attributed to two simultaneous effects: the thermal expansion of the weakened flame at reduced flow, which shortened the distance between the flame front and the radiometers, and the accumulation of hot combustion products within the chamber resulting from the lower flow rate.

Combined with the absence of spread discussed above, flame growth on thick materials in low-gravity is very different from normal-gravity. The growth rate trends for the 2-sided samples show a 73% increase in the spread rate from an oxygen concentration increase of 0.08 mol fraction despite the overall pressure decrease of 45%. For the 1-sided samples growth rate was unchanged for an oxygen increase of 0.03 mol fraction with a pressure decrease of 27%.

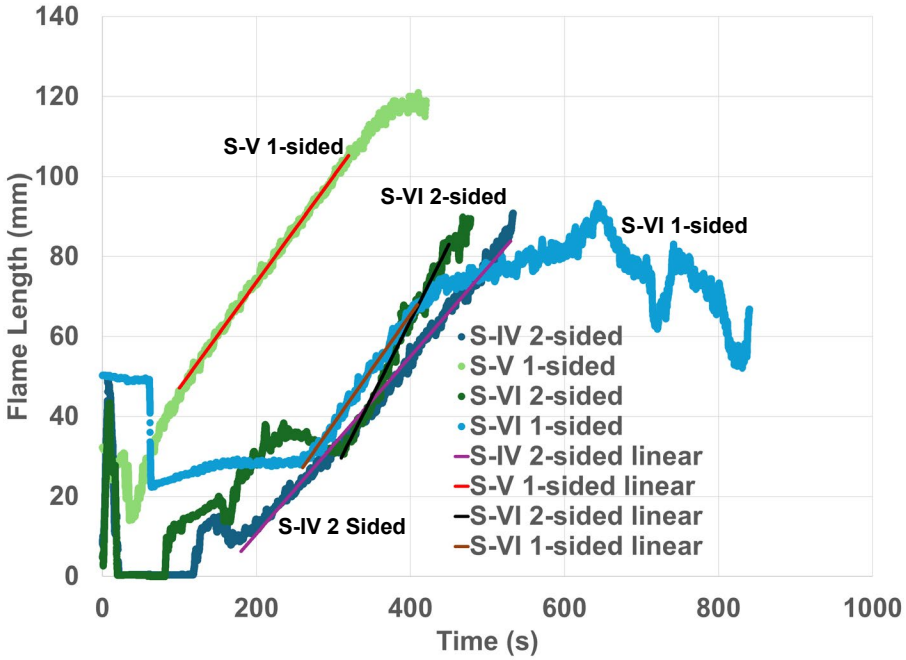


Figure 5. Flame length versus time for the 4 PMMA tests. The time is adjusted to each test to start when the ignitor was turned off. Plotted with each trace is the linear fit to the steady growth period. The test conditions are given in Table 1.

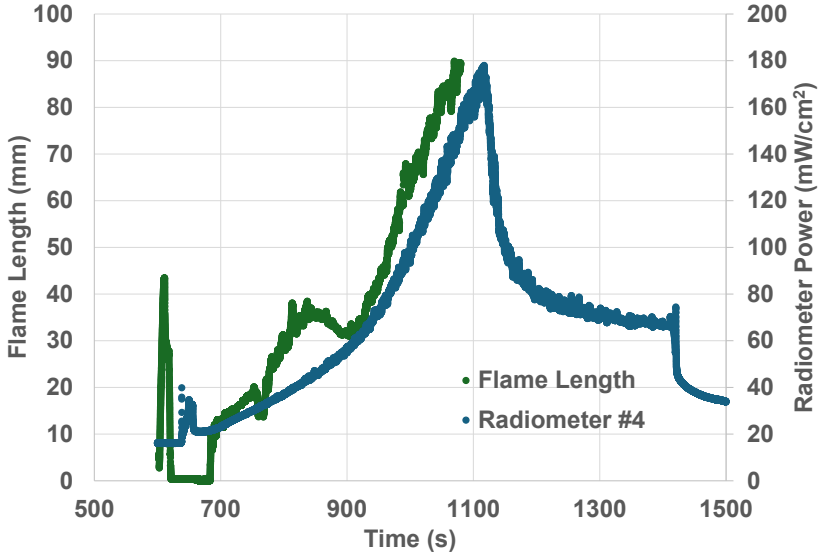


Figure 6. Flame length and radiometer signal for the SAFFIRE VI 2-sided sample. Flame tracking was stopped when the flow reduction began because the flame shrank substantially.

In Figure 7 the smoke aerosol detected at the FFD tracks the flame length with a minor delay. This limited delay is likely due to the direct path from the SFU to the FFD. Even though they were on opposite ends of the Cygnus module, the bulk of the flow went directly to the FFD without the extensive mixing seen in geometries like the ISS [12]. Consequently, the detection scenario tested here is likely to be quicker than in many spacecraft. Figure 8 compares the HRR from the fire with the radiometer for the same 2-sided test in SAFFIRE VI. The peak HRR hit 3 kW which is substantial for a small spacecraft. However, as seen in Table 1, the temperature rise at the FFD was only 0.5 °C. Larger temperatures (peak of 77 °C) were seen at the outlet of the SFU [9] but they quickly reduced due to mixing and heat loss.

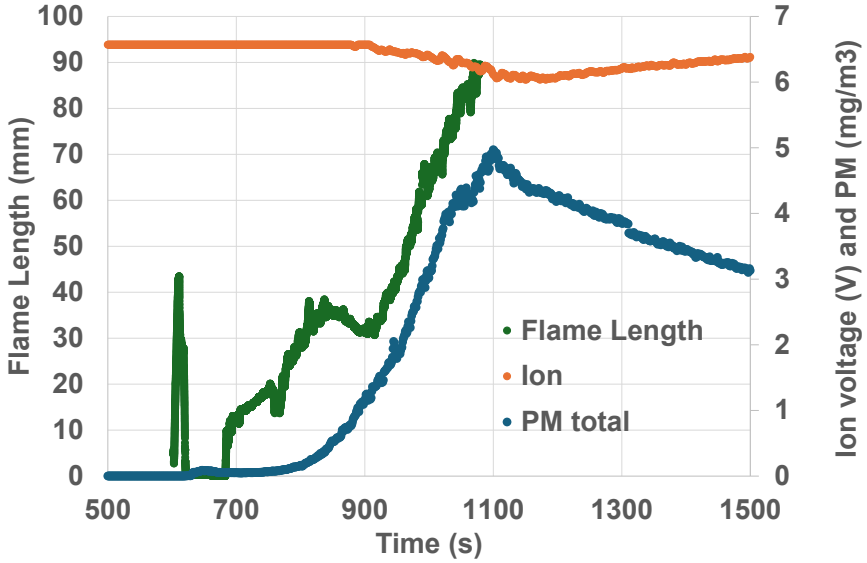


Figure 7. Flame length, FFD Ionization smoke detector signal and the total particulate matter (PM total) measured by the DustTrak DRX for the SAFFIRE VI 2-sided sample. The ionization chamber voltage decreases as aerosol concentration increases.

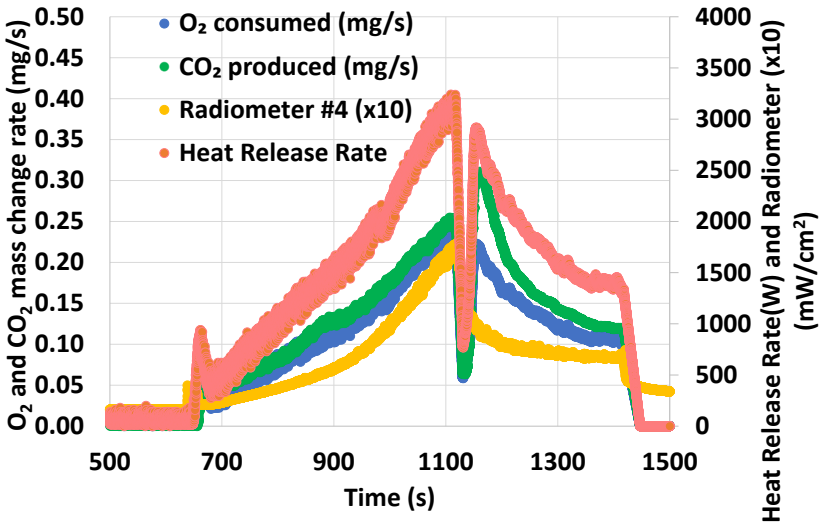


Figure 8. Heat release rate and species production/consumption during SAFFIRE VI 2-sided PMMA sample.

The SAFFIRE configuration in the spacecraft had no method to remove CO and only limited capacity to remove CO_2. As a result, for all but the first test, there was an existing baseline level of these gases. The data are reported in Table 1 as the increase in CO and CO_2 for each test rather than the absolute value. The 1-hour limit for CO_2 and the 24-hour SMAC for CO were exceeded by the maximum increase for both PMMA tests on SAFFIRE VI. In addition, the 24-hour SMAC for CO was exceeded on SAFFIRE IV for PMMA and for SIBAL on SAFFIRE VI. The high levels for the SAFFIRE VI PMMA and SIBAL cases were likely due to the higher oxygen concentrations for those tests.

Instead of the peak value, the more important measure is the concentration of hazardous products at the time the fire is detected. Ideally, the fire detection threshold should be determined such that, for the expected possible fires in the spacecraft, the detection system will detect the fire in time for the crew to effectively respond to the fire. To

examine this question, an alarm threshold of 2 mg/m^3 of total particulate matter detected by the TSI DustTrak DRX in the FFD was used as a reference point (see Fig. 7 for an example). The time to achieve this concentration is tabulated in Table 1 along with the increase in CO_2 and CO at that time interval. Also tabulated are the flame length and the HRR at detection. This detection threshold detected the fire before the SAFFIRE IV PMMA sample and SAFFIRE VI SIBAL sample reached hazardous CO levels however both PMMA samples from SAFFIRE VI exceeded the CO threshold with the 1-sided sample approaching the 1-hour SMAC. Notably the CO increase was worse for the 1-sided sample. The SAFFIRE VI results suggest that a lower threshold or additional detectors would be needed for this spacecraft configuration.

IV. Conclusion

Overall, the SAFFIRE IV-VI test series provided useful validation that flame growth rate for flat materials can be expected to exhibit linear growth without the acceleration seen in 1-g. This fact is extremely significant when considering the timeline of the response to a spacecraft fire. In the case of the 1-sided PMMA samples, this growth reached a limiting size which is even more significant. It is possible that the 2-sided samples were not burned long enough to reach a limiting size.

For this configuration spacecraft, a 2 mg/m^3 detection threshold was not low enough to detect the fires before some cases exceeded the 24-hour SMAC for CO, however it only approached the 1-hour SMAC for one case. These results suggest that implementing smoke detection in this spacecraft for these design fires would require either a lower threshold or additional smoke detectors to reduce the transport time. Proper selection of fire detection and response systems depends on the ability to assess whether the smoke detector can identify a fire before the spacecraft is uninhabitable. An assessment of this would require analysis specific to the spacecraft volume and flow conditions using heat and smoke production data such as this in a model of the planned spacecraft.

Acknowledgments

The authors acknowledge the support of the NASA Mars Campaign Office, for the sponsorship of the Spacecraft Fire Safety Demonstration Project and the SAFFIRE experiments. In addition, the authors acknowledge the support of the various space and research agencies that have supported this work including but not limited to the Japan Aerospace Exploration Agency (JAXA), the European Space Agency, the Russian Space Agency, the National Centre for Space Studies (CNES), the German aerospace Center (DLR), the European Union, the Russian Science Foundation, and NASA. Grunde Jomaas and Ulises Rojas Alva are supported by FRISSBE project, which has received funding from the European union's Horizon 2020 research and innovation program under Grant Agreement No. 952395. The excellent support from the engineering team (NASA and Zin Technologies), Northrup Grumman and the on-orbit crew are gratefully acknowledged.

References

[1] P. Ferkul, S. Olson, D. Urban, G. Ruff, J. Easton, J. T'ien, Y.-T. Liao, C. Fernadez-Pello, J. Torero, C. Eigenbrod, G. Legros, N. Smirnov, O. Fujita, S. Rouverau, B. Toth and G. Jomaas, "Results of large-scale spacecraft flammability tests.," in *47th International Conference on Environmental Systems, ICES-2017-224*, 2017.

[2] D. Urban, P. Ferkul, S. Olson, G. Ruff, J. Easton, J. T'ien, Y. Liao, C. Li, C. Fernandez-Pello, J. Torero, G. Legros, C. Eignebrod, N. Smirnov, O. Fujita, S. Rouvereau, B. Toth and G. Jomaas, "Flame spread: Effects of microgravity and scale," *Combustion and Flame,* vol. 199, pp. 168-182, 2019.

[3] S. Olson, D. Urban, G. Ruff, P. Ferkul, B. Toth, C. Eigenbrod and F. Meyer, "Analysis of Saffire II two-sided concurrent flame spread over a thick PMMA slab," in *48th International Conference on Environmental Systems, ICES-2018-101*, 2018.

[4] C. Eigenbrod, F. Meyer, G. Jomaas, D. Urban, G. Ruff, S. Olson, P. Ferkul and B. Toth, "Eigenbrod, C., Meyer, F., Jomaas, G., Urban, D. L., Ruff, G. A., Olson, S., Ferkul, P., and Toth, B.,Opposed flame spreading along a structured PMMA sample in exploration atmosphere under microgravity," in *50th International Conference on Environmental Systems, ICES-2021-244*, 2021.

[5] S. Olson, D. Urban, G. Ruff, P. Ferkul, B. Toth, C. Eigenbrod, F. Meyer and G. Jomaas, "Concurrent flame spread over two-sided thick PMMA slabs in microgravity," *Fire Technology,* vol. 56, pp. 49-69, 2020.

[6] D. Urban, G. Ruff, P. Ferkul, J. Easton, J. Owens, S. Olson, C. Fortenberry, J. Brooker, J. Graf, M. Casteel, B. Toth, F. Meyer, C. Eigenbrod, J. T'ien, Y.-T. Liao, C. Fernandez-Pello, G. Legros, A. Guibaud, N. Smirnov, O. Fujita and G. Jomaas, "Fire Safety Implications of Preliminary Results from Saffire IV and V Experiments on Large Scale Spacecraft Fires," in *50th International Conference on Environmental Systems, ICES-2021-266*, 2021.

[7] C. Fortenberry, M. Casteel, J. Graf, J. Easton, J. Niehaus, M. Meyer, D. Urban and G. Ruff, "Evaluation of Combustion Products from Large-Scale Spacecraft Fires during the Saffire-IV and Saffire-V Experiments," in *50th International Conference on Environmental Systems, ICES-2021-244*, 2021.

[8] J. Niehaus, J. Brooker, D. Urban and G. Ruff, "Vehicle Modeling during the Burning of Thermally Thick Samples in the Saffire V Experiments," in *53rd International Conference on Environmental Systems, ICES-2024-310*, 2024.

[9] D. Urban, G. Ruff, P. Ferkul, J. Easton, M. Johnston, O. J. Owens, Sandra, C. Fortenberry, J. Graf, O. George, B. Toth, F. Meyer, C. Eigenbrod, J. T'ien, Y.-T. Liao and C. Fernandez-Pello, "Preliminary Results from the Saffire VI Experiment," in *53rd International Conference on Environmental Systems, ICES-2024-365*, 2024.

[10] NASA JSC, "Spacecraft Maximum Allowable Concentrations for Airborne Contaminants, JSC 20584, Revision A,," NASA JSC,, Houston TX., 2020.

[11] NASA JSC, "Nasa Spaceflight Human-System Standard Volume 2: Human Factors, Habitability, And Environmental Health, NASA-STD-3001, Volume 2, Revision D,," NASA JSC, Houston TX., 2023.

[12] J. Brooker, D. Urban and G. Ruff, "ISS Destiny Laboratory Smoke Detection Model," in *37th International Conference On Environmental Systems, 2007-01-3076*, Chicago, IL, 2007.

[13] A. C. Fernandez-Pello and T. Hirano, "Controlling mechanisms of flame spread," *Fire Science and Technology,* vol. 2, no. 1, pp. 17-54, 1982.